1984A&A...131..333S

Astron. Astrophys. 131, 333–346 (1984)

ASTRONOMY AND ASTROPHYSICS

Diagnostics of solar magnetic fluxtubes using a Fourier transform spectrometer

J. O. Stenflo[1], J. W. Harvey[2], J. W. Brault[2], and S. Solanki[1]

[1] Institute of Astronomy, ETH-Zentrum, CH-8092 Zürich, Switzerland
[2] Kitt Peak National Observatory*, P.O. Box 26732, Tucson, AZ 85726, USA

Received August 31, accepted October 5, 1983

Summary. Circularly polarized spectra have been recorded in plages and a network element near disk center, using the Fourier transform spectrometer (FTS) at the Kitt Peak McMath telescope as a polarimeter. The spectra are fully resolved, and cover about 2000 Å in the visible with high signal-to-noise ratio. An overview of the diagnostic contents of these spectra for the modelling of small-scale magnetic fluxtubes is presented. The data admit a determination of the height variation of the various spatially unresolved fluxtube parameters, like intrinsic field strength, relative cross-sectional area, velocities, thermodynamic properties, etc.

Particular attention is payed to the strong asymmetries in the Stokes V profiles, which are inconsistent with magnetohydrostatic models, but require height gradients of a velocity field. If the V profiles had not been fully spectrally resolved, the V asymmetry would have caused an apparent redshift of the V profile, leading to fictitious downdrafts in the fluxtubes.

It is further shown how empirical Landé factors can be obtained, to test the validity of LS coupling or to be used for line identifications.

Key words: solar magnetic fields – fluxtubes – Fourier transform spectrometer – Stokes parameters

1. Introduction

Solar magnetic fields are measured by recording the Zeeman-effect polarization in selected spectral lines. There are two main avenues in determining the properties of the magnetic fine structures:
(a) Polarization recordings with increased spatial resolution.
(b) Using spectral information to become independent of the spatial resolution.

The "brute-force" method (a) has the disadvantage that one can never be sure that the features have been fully resolved. With advances in the attainable resolution, the apparent field strength measured has been increasing.

The spectral methods (b) have the advantage that the field strengths and other properties measured become instrument-independent, unaffected by the low spatial resolution actually used. The situation is analogous to using spectral line widths to obtain information on the turbulent and thermal microscopic velocities, whereby the spatial resolution used has nothing to do with the actual size of the moving elements. Similarly, for the magnetic fine structures, the spatial resolution has little to do with the sizes of the much smaller fluxtubes.

The disadvantage of the spectral methods is however that they only provide us with statistical properties, with no information on morphology and evolution. Fortunately, the solar magnetic fluxtubes appear to have "unique" properties, in the sense that the statistical spread in their parameters, e.g. field strengths, appears to be quite small, even if we compare fluxtubes from active-region plages with those of the quiet-region network (Stenflo, 1976). This remarkable "uniqueness" of the fluxtube properties dramatically enhances the power of the spectral methods, since the determined characteristics will be quite well defined although the method is statistical in nature.

A second disadvantage of the spectral methods is some model dependence, but this can be reduced to a minimum and practically eliminated by a careful combination of spectral parameters.

In the past, the spectral method has been mainly limited to the line-ratio technique in solar work, whereby the Zeeman-effect polarization is recorded simultaneously with a Babcock-type magnetograph in the wings of two suitably chosen spectral lines (Stenflo, 1973, 1976; Harvey, 1977). Another important spectral method is the Robinson technique, which has become a major tool to determine the magnetic fine structure on the surfaces of other stars (Robinson et al., 1980; Marcy, 1983).

Over a number of years, attempts have been made to extend the spectral information by recording polarized line profiles (e.g. Harvey et al., 1972; Baur et al., 1980). These attempts have been hampered by the limited speed of grating spectrometers when pushing for both high spectral resolution and photometric accuracy.

With the modification of the Fourier transform spectrometer (FTS) of the Kitt Peak McMath telescope into a polarimeter (Brault, 1978; Stenflo et al., 1983b), a breakthrough in Stokes polarimetry and in the spectral methods of magnetic-field diagnostics has been achieved. The FTS is superior in speed, spectral resolution, and wavelength coverage as compared with a grating spectrometer. The polarized spectrum can be completely spectrally resolved, and does not contain any straylight.

With previous instruments it had not been possible to record even a single polarized line profile with a resolution and signal-to-noise ratio comparable to that of the FTS. With our present FTS observations, all the many hundreds of spectral lines within the 1000 Å prefilter pass band have been recorded with this high

Send offprint requests to: J. O. Stenflo

* Operated by the Association of Universities for Research in Astronomy, Inc., under contract with the National Science Foundation

© European Southern Observatory • Provided by the NASA Astrophysics Data System

1984A&A...131..333S

Table 1. FTS spectra of Stokes I and V

Date (1979)	Solar feature	Wavelength range (Å)	Spectral resolution	Integration time (min)
April 30	Strong plage	4524–5580	420000	35
		5254–6907	500000	21
April 29	Weak plage	4566–5580	420000	52
April 30	Enhanced network	4104–4942	360000	69
		5254–6907	500000	57

precision strictly simultaneously. We are thus not limited to using combinations of two or three lines as with the line-ratio technique, but can make use of a much larger number of lines to provide simultaneous constraints on the fluxtube models, similar to the use of 402 unblended Fe I lines by Stenflo and Lindegren (1977) to constrain their model of line broadening by magnetic turbulence. The lack of spatial information is thus compensated for by superb information in the spectral domain.

It may be noted that two-dimensional images with high spatial resolution can also be recorded with the FTS, giving a resolved spectrum at each spatial pixel element. This is in contrast to grating spectrometers, which only provide one-dimensional spatial information (without spatial scanning).

In the present paper we will present an overview of the diagnostic contents for fluxtube modelling of the FTS recordings of the longitudinal Zeeman effect that we made in April 1979.

2. Observations and data reduction

The set-up used to record the polarized spectrum with the FTS at the Kitt Peak McMath telescope has been described in Stenflo et al. (1983b). The technique was first outlined by Brault (1978). A KD*P crystal in front of the FTS modulates the circular polarization at 10 kHz, but since the FTS acts in itself as a modulator, a fairly sophisticated detection scheme including a heterodyning technique had to be developed, to map the polarized and unpolarized spectra into different portions of the available frequency domain. 1000 Å prefilters were used. All wavelengths within the prefilter passband are recorded strictly simultaneously for each Fourier component. A scan in the Fourier domain takes about 7 min to reach a spectral resolution of 500000 in the green portion of the spectrum, and is normally repeated to enhance the signal-to-noise ratio. While all wavelengths are simultaneously observed, the frequency components that constitute the spectral line structure are not sampled simultaneously. This permits the possibility of line profile distortion if the properties of the observed solar region change during a scan. The five-minute photospheric oscillation is a particularly dangerous possibility. We tried to minimize this possibility by integrating over several oscillations and by using a scan time different from 5 minutes.

The entrance aperture (spatial resolution) was a 4 mm diameter (= 10 seconds of arc) circular hole. Since, as explained in the introduction, the spectral method of fluxtube diagnostics is independent of spatial resolution as long as the resolution element is much larger than the subarcsec fluxtubes, there would in general be no gain in diagnostic power by reducing the resolution element to say one sec of arc, only a probable loss in signal-to-noise ratio and a higher sensitivity to seeing fluctuations. With our resolutions and integration times, a noise level in the degree of circular polarization as low as about 0.01% could be reached.

The recordings described were made on April 29–30, 1979, and are summarized in Table 1. Only features near the center of the solar disk were selected. When judging the spectral resolution, it should be remembered that the modulation transfer function (MTF) is unity out to the given spectral resolution. This is in contrast to grating spectrometers, for which the MTF tapers off gradually. From viewing the corresponding interferograms, one could see that in the green portion of the spectrum, for instance, there is not much information in the solar spectrum beyond a resolution of 250000, so our spectra are actually "overresolved". For all practical purposes, the width of the instrumental function can be regarded as zero.

The unpolarized spectra were contaminated by weak interference fringes, in particular at the shorter wavelengths, caused by the KD*P modulator. Using numerical fits with a Fabry-Perot equation, the fringes could be successfully removed in the data analysis.

The instrumental circular polarization was compensated for by introducing a phase retardation with a Soleil compensator in front of the KD*P modulator. The phase retardation was adjusted until the DC component of the demodulated FTS signal read zero. As the telescope phase retardation varies slowly with wavelength within the prefilter range, a small remaining zero-line error is unavoidable. Although it cannot be compensated for in real time, it can be eliminated in the data analysis.

The solar spectral features in V/I (degree of circular polarization) are not significantly distorted by telescope retardation or polarization apart from an additive false zero level, since the $V-I$ cross-talk term is very small when V/I is also small (as is the case in our data). Accordingly, it is easy to subtract out this background. The true zero level is found assuming that V/I should be zero in the continuous spectrum (or, in our practical calculations, for the points with $0.98 \leqq I/I_c \leqq 1$, where I_c is the continuum level). This is a safe assumption considering that we are working near disk center with a 10 seconds of arc entrance aperture.

It is important to note that the zero-line correction must be applied to the V/I data, not to the undivided Stokes V, since the instrumental polarization contains the solar spectral features in V (but not in V/I, cf. the analysis in Stenflo et al., 1983a). For comparison with theory it is however more useful to work with the undivided V. After the zero-line correction of the V/I data, we have therefore multiplied by the I spectrum to obtain our final V spectrum, normalized to I_c, the intensity of the continuous spectrum.

Polarization calibration was achieved by making an FTS recording with a circular polarizer (linear polarizer + Fresnel romb) in front of the modulator. Our previous analysis of the FTS

© European Southern Observatory • Provided by the NASA Astrophysics Data System

1984A&A...131..333S

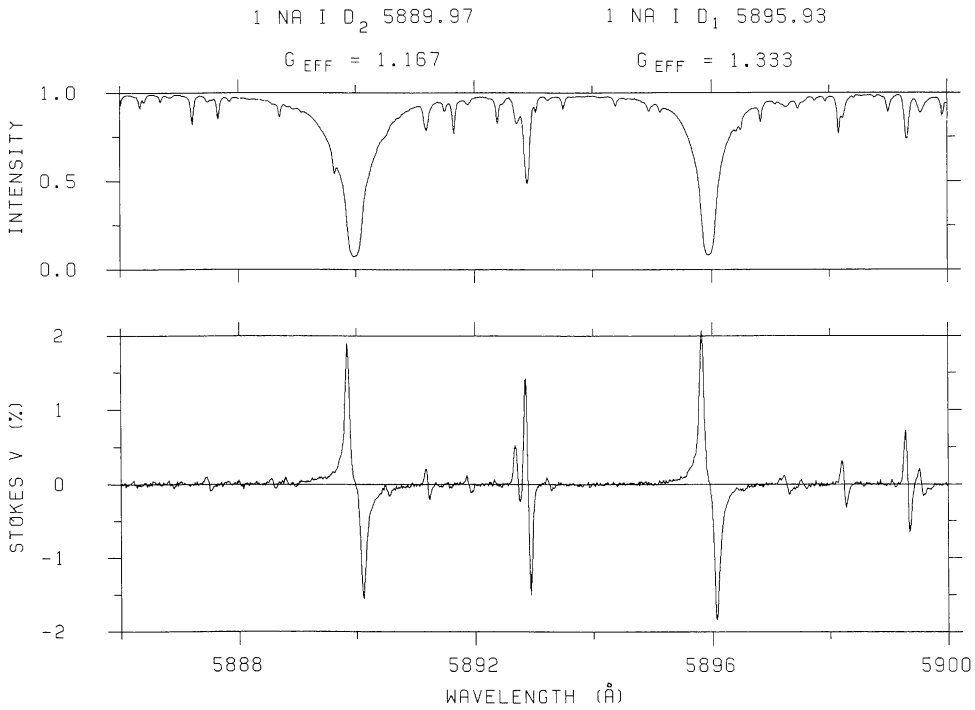

Fig. 1. Stokes I and V around the Na I D_2 and D_1 lines, recorded in a strong plage near disk center. Stokes V is given in units of the intensity of the adjacent continuum

linear polarization data indicates that the polarization scale may be too low by as much as a factor of two (Stenflo et al., 1983b), although it is hard to believe that the telescope depolarization (which escapes the calibration procedure) could be that high. We do not know if the same problems apply to the circular-polarization data as well, but it may be wise to use the polarization scale with some care.

With the present observational material for fluxtube diagnostics, we have at our disposal atlases of the spectrally fully resolved I and V spectra, covering 2000–3000 Å, both in an active-region plage and in the enhanced quiet-sun network.

3. Diagnostic contents of the polarized line profiles

There are numerous facets to the problem of interpreting the polarized line profiles, and the treatment can be done at many different levels of sophistication, with various approximations involved. The observational material provided by the FTS is overwhelming in its richness. In the following, we will present an overview of the diagnostic contents of the FTS spectra for fluxtube modelling, to identify the relevant parameters and to indicate how the information can be extracted.

3.1. Weak-field model

As our first example of a Zeeman-effect recording with the FTS, we show in Fig. 1 the region around the Na I D_1–D_2 lines, recorded in a strong plage. Let us first consider the question what it is that determines the characteristic anti-symmetric shape of the Stokes V profiles.

To illuminate the physics we start off with the simple-minded assumption that the magnetic field is vertical and homogeneous over the resolution element. Consider also for simplicity a normal Zeeman triplet. The line is then split by the magnetic field B into two σ components with opposite circular polarization. Their intensities are

$$I_{\sigma_{1,2}}=\tfrac{1}{2}(I\pm V)\,. \tag{1}$$

Accordingly, the V profile is simply

$$V=I_{\sigma_1}-I_{\sigma_2}\,. \tag{2}$$

The next crucial step is that the simple relation

$$I_{\sigma_{1,2}}(\lambda)=\tfrac{1}{2}I(\lambda\pm\Delta\lambda_H) \tag{3}$$

can be shown (see below) to be valid independent of the magnitude of the Zeeman splitting $\Delta\lambda_H$. Due to this remarkable circumstance, a Taylor expansion of (3) combined with (2) gives us

$$V=\Delta\lambda_H\frac{\partial I}{\partial\lambda}+\ldots\,, \tag{4}$$

where the terms containing higher derivatives of I can be neglected when the splitting $\Delta\lambda_H$ is much smaller than the width of the spectral line (weak-field approximation). The Zeeman splitting is

$$\Delta\lambda_H=4.67\,10^{-13}g\lambda^2B\,, \tag{5}$$

where g is the Landé factor, B should be given in G, and the wavelength in Å.

Although we have considered the case of a normal Zeeman triplet for simplicity, it is straightforward to generalize to any anomalous Zeeman splitting pattern, arriving again at (4) if g in (5) is replaced by $g_{\rm eff}$, the effective Landé factor defined and tabulated by Beckers (1969).

Let us now test the prediction of (4) that V and $\partial I/\partial\lambda$ should be proportional to each other, by plotting in Fig. 2 V and $\partial I/\partial\lambda$ for the Na I D_1 line. $\partial I/\partial\lambda$ has been normalized to the positive amplitude

© European Southern Observatory • Provided by the NASA Astrophysics Data System

1984A&A...131..333S

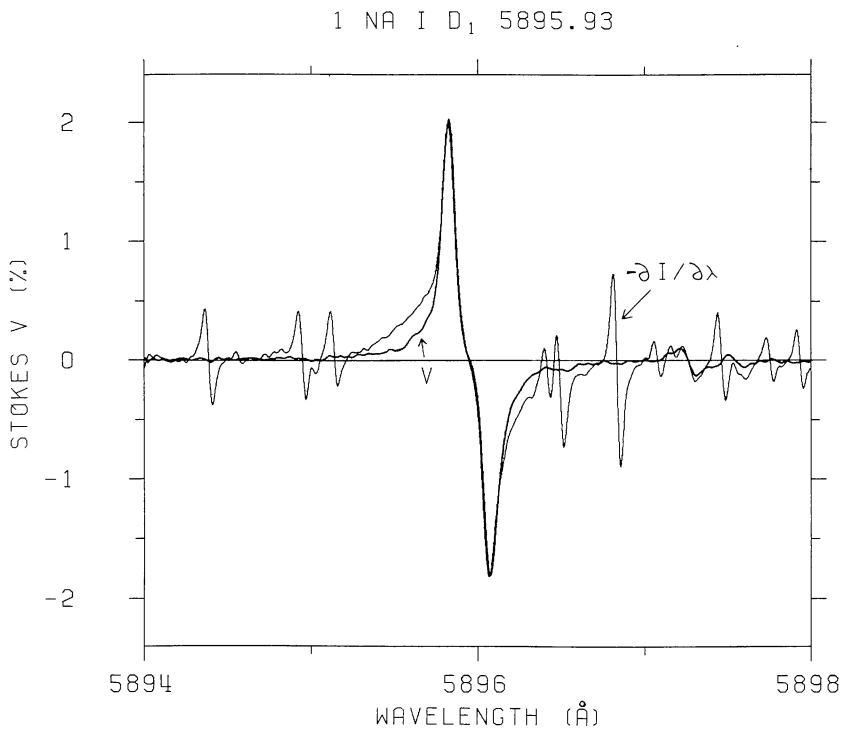

Fig. 2. Stokes V *(thick curve)* and intensity gradient $\partial I/\partial\lambda$ *(thin curve)* around the Na I D_1 line, using the same data as in Fig. 1. $\partial I/\partial\lambda$ has been multiplied by 4.3 mÅ to normalize its amplitude to that of Stokes V. Notice the strong water vapor components in $\partial I/\partial\lambda$, which are absent in Stokes V

of V. The agreement between V and $\partial I/\partial\lambda$ is almost perfect within the D_1 line, but becomes bad in the far wings and outside the line due to the large contribution from terrestrial water vapor, which of course does not contribute to the circular polarization (see Sect. 3.2 below). As the D_1 line is so broad, the weak-field model (neglecting the higher-order terms in the Taylor expansion) is a good approximation, even when we have to deal with intrinsic field strengths of the order of 1 kG.

The normalization factor for $\partial I/\partial\lambda$ in Fig. 2 is 4.3 mÅ, and is simply equal to $\Delta\lambda_H$ according to (4). Using (5) with $g_{\text{eff}}=1.33$, we obtain $B=200$ G. If we would go from our homogeneous one-component model to a two-component model with a fraction α of the surface being covered by fields of strength B, the remaining portion $1-\alpha$ being field-free, our discussion would remain the same, except that B would have to be replaced by αB.

Another example of a broad line, for which the weak-field approximation is certainly appropriate, is the Hβ line in Fig. 3. In Fig. 4 we compare again V and $\partial I/\partial\lambda$, normalized to the negative V amplitude of Hβ (in the blend-free line wing). Again we find an excellent agreement within the Hβ line itself, the deviations coming

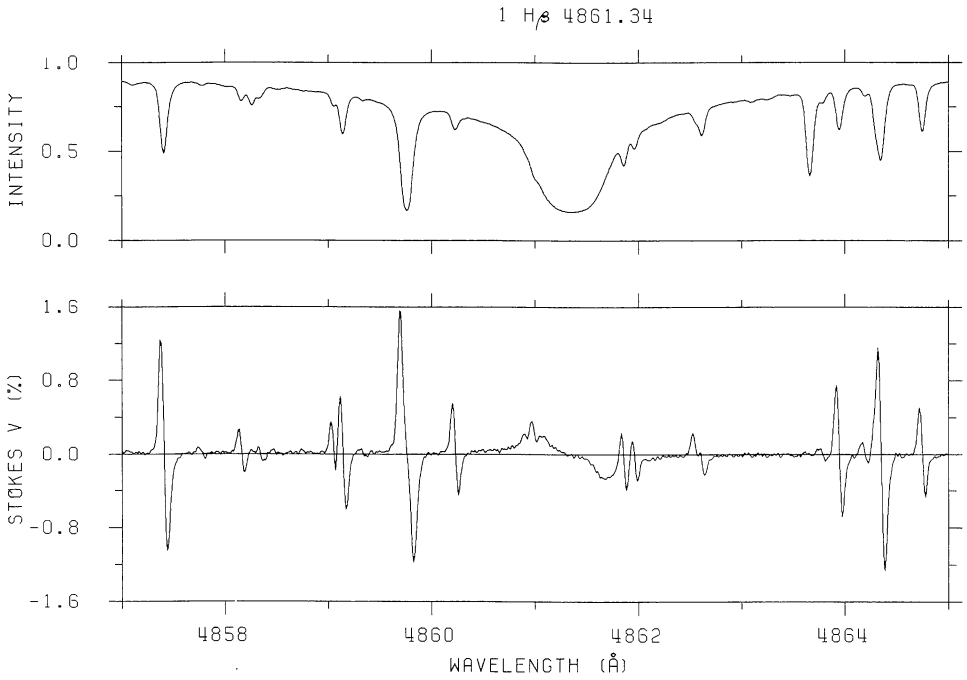

Fig. 3. Stokes I and V around the Hβ line, recorded in a strong plage near disk center

© European Southern Observatory • Provided by the NASA Astrophysics Data System

1984A&A...131..333S

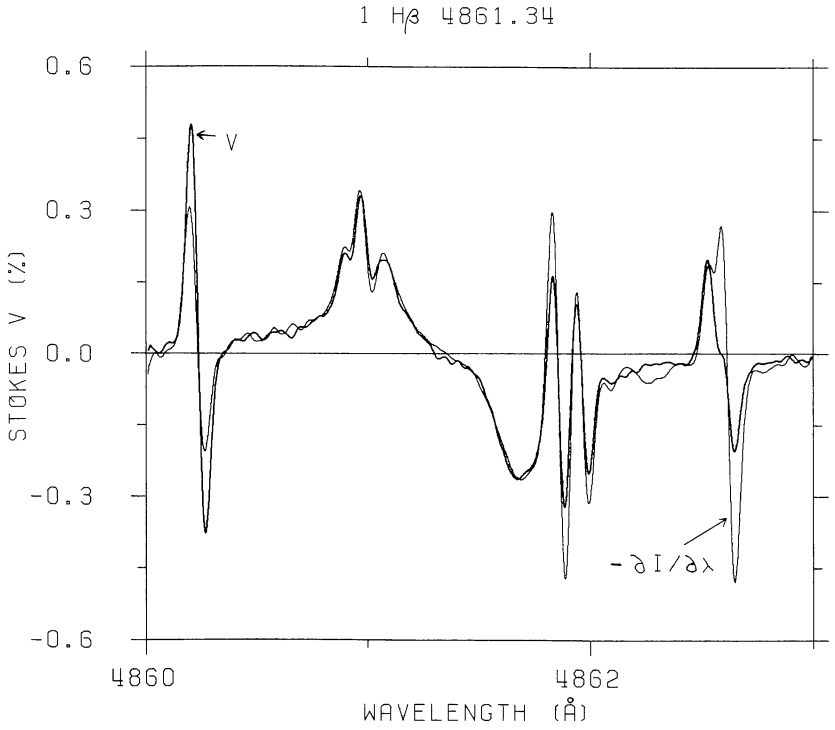

Fig. 4. Stokes V *(thick curve)* and $\partial I/\partial\lambda$ *(thin curve)* around Hβ, using the same data as in Fig. 3. $\partial I/\partial\lambda$ has been multiplied by 1.8 m Å to normalize the amplitude in the red Hβ line wing to that of Stokes V

mainly from blend lines and noise ripples. Since the other lines in the range have different Landé factors, the Hβ normalization does not apply to them, which causes the large discrepancies between V and $\partial I/\partial\lambda$ outside the Hβ line.

Let us now go back to the remarkable equation (3) and explain why it is valid for any Zeeman splitting and any stellar atmosphere. It works because the two σ components have mutually orthogonal polarization states. It can be shown (Chandrasekhar, 1950) that two beams, I_+ and I_-, of mutually orthogonal polarization states cannot interact with each other; an atmosphere that absorbs I_+ is completely transparent to I_-, and vice versa. In general any elliptical polarizations can be considered, but with our choice of field direction, I_+ and I_- correspond to left- and right-handed circular polarization.

Because of this property of orthogonally polarized beams, it is possible to diagonalize the Mueller matrix for radiative absorption. In the Unno (1956) formulation of the radiative transfer problem in a magnetic field, the various parameters are hopelessly mixed, since the Stokes parameters are based on a system of linear polarization vectors, which in general does not correspond to the polarization states of the σ and π components. This makes the absorption matrix highly non-diagonal. By choosing a suitable polarization basis, however, the polarization matrix diagonalizes, corresponding to the decoupling of beams of mutually orthogonal polarization states.

The diagonalized formulation of the transfer problem was first introduced by Stepanov (1958a, b), and was extended by Rachkovsky (1961a, b). In the review of Stenflo (1971), the relations between the different formulations have been clarified, and the diagonalization transformation has been explicitly given.

The above discussion applies to any stellar atmosphere and radiative-transfer problem, as long as the source function does not contain a scattering matrix that does not diagonalize with the absorption matrix and therefore may mix the polarization states, and as long as magnetooptical effects are unimportant. In the special case of a longitudinal magnetic field that we have considered, magnetooptical effects do not enter at all.

When looking at the analytical solutions of the transfer equations including magnetooptical effects given by Eq. (45) in Stenflo (1971), the σ components seem to be mixed in a number of quadratic terms, but if one carries out some algebraic manipulations of the expressions (we leave this to the interested reader), the expressions for I and V condense out to yield the beautifully simple (3).

3.2. *Telluric lines and blends*

The circularly polarized spectrum can be quite useful for the identification of weak spectral lines and blends, as was noted when Figs. 1–4 were presented above. First of all the Stokes V spectrum is considerably "cleaner" than the I spectrum, since it is entirely free from telluric components. This is very conspicuous in Fig. 2, where the numerous lines of atmospheric water vapor stand out in $\partial I/\partial\lambda$ with respect to the smooth V curve.

Weak blend lines of solar origin show up well in both V and $\partial I/\partial\lambda$ as illustrated in the blue wing of Hβ (Fig. 4). However, the V spectrum introduces a new constraint on possible line identifications by requiring the predicted and observed polarization amplitudes to match. From the ratio between the $\partial I/\partial\lambda$ and V amplitudes the empirical Landé factor of the line can be determined, regardless of whether the line has been identified or not. A candidate atomic transition has to have that Landé factor. This technique implicitly presumes that the unidentified line is formed in the same magnetic field as identified lines.

© European Southern Observatory • Provided by the NASA Astrophysics Data System

1984A&A...131..333S

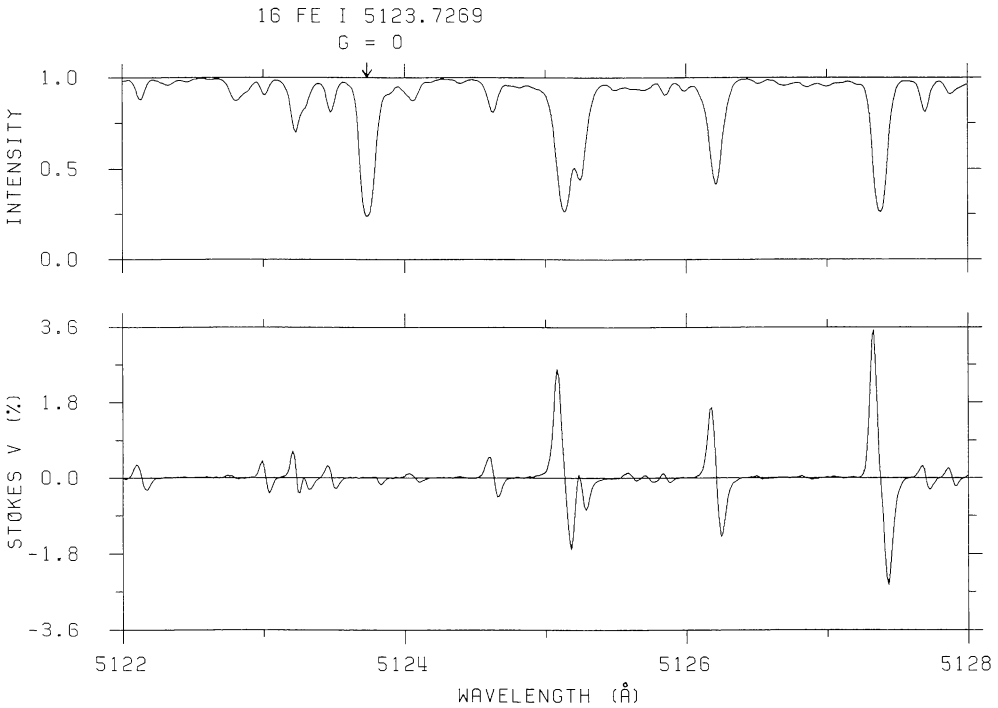

Fig. 5. Stokes I and V recording in a strong plage near disk center, illustrating the absence of polarization in the line 16 Fe I λ5123.73 Å with a Landé factor of zero

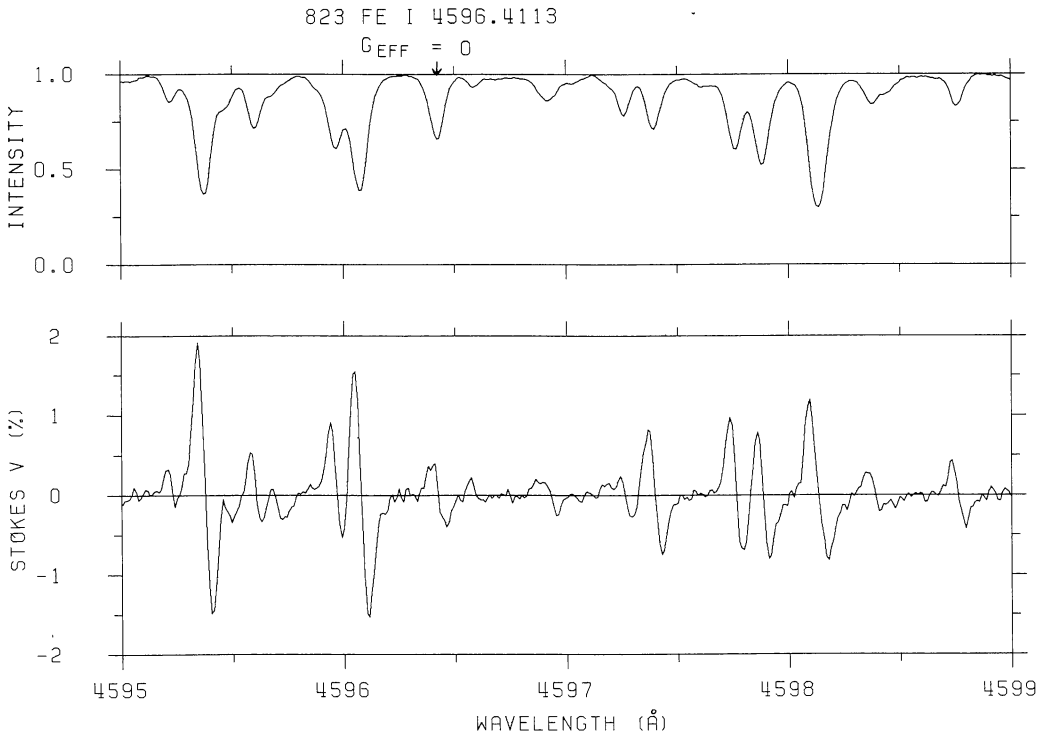

Fig. 6. Stokes I and V recording in a strong plage near disk center, illustrating the failure of LS coupling for the line 823 Fe I λ4596.41 Å. The clear polarization signature shows that the true effective Landé factor must be positive, although LS coupling predicts it to be zero

3.3. Validity of LS coupling

In the preceding sections we have seen how a comparison of $\partial I/\partial\lambda$ with V leads to determinations of empirical Landé factors. In this way the sun may serve as an atomic physics laboratory, allowing the theoretically calculated Landé factors to be checked. Let us at this point add the warning that the physics of fluxtubes must be properly accounted for, otherwise there may be large systematic errors in the derived empirical Landé factors, as will be obvious from the following sections.

We can however present some qualitative examples of this type of atomic physics without having to deal with fluxtube effects. The

© European Southern Observatory • Provided by the NASA Astrophysics Data System

1984A&A...131..333S

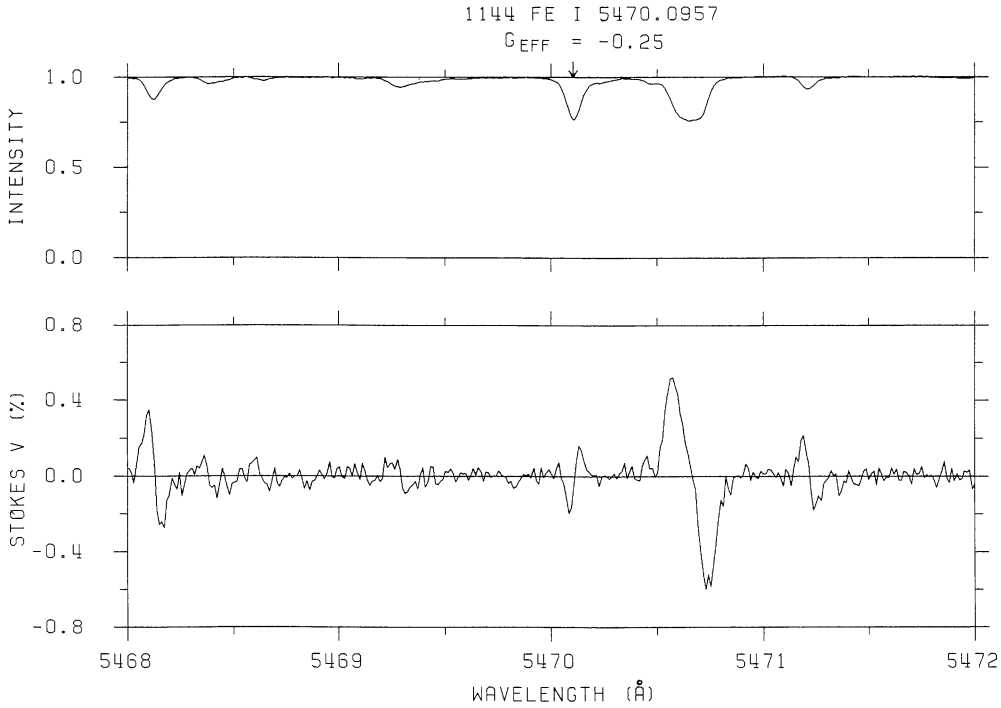

Fig. 7. Stokes I and V recorded in a strong plage near disk center, illustrating how the line 1144 Fe I λ5470.10 Å has a polarization signature of reversed sign, in agreement with the prediction based on LS coupling

standard means of obtaining a Landé factor for an identified line has been to use the L, S, and J quantum numbers in the LS coupling formula. Thus the tabulation of Beckers (1969) is based on LS coupling. Considerable deviations from the LS coupling scheme are however relatively frequent, in particular in Fe I, where the states are partially mixed. j–j coupling is sometimes a better approximation.

To illustrate some clear cases when LS coupling works, and when it does not work, we have selected a few lines with zero or negative LS Landé factor, using the Fe I list of Stenflo and Lindegren (1977). Figure 5 shows the strong non-magnetic line 16 Fe I λ5123.7 Å. In contrast to the surrounding lines, its anti-symmetric V profile is strikingly absent, illustrating that LS coupling works well in this case.

Figure 6 shows an example where the LS coupling prediction of a vanishing Landé factor does not work. The line 823 Fe I λ4596.4 Å shows a V polarization signature typical of a line with a positive Landé factor, although the effective LS coupling Landé factor, calculated according to the formulae in Beckers (1969), is zero.

Landi Degl'Innocenti (1982) has recently calculated the effective Landé factor of the 4596.4 Å line, using the experimental Landé factors of the lower and upper levels. He finds $g_{\rm eff} = 0.753$, which is in agreement with our results, demonstrating the failure of LS coupling for this line.

In a few very rare cases the LS coupling Landé factor is negative. One would then expect that the sign of the Stokes V profile would reverse with respect to the other surrounding lines of positive Landé factor. Figure 7 shows a line for which this is really the case: 1144 Fe I λ5470.1 Å with $g_{\rm eff} = -0.25$.

A conspicuous case where this sign reversal does not take place is shown in Fig. 8. The polarization signature of the line 1177 Fe I λ6094.4 Å with $g_{\rm eff} = -0.25$ clearly corresponds to a line with positive Landé factor. If we use the neighbouring line of the same multiplet, 1177 Fe I λ6093.6 Å, as a reference, and adopt its LS Landé factor of 0.333 to determine the value of αB of the average magnetic field, a comparison between V and $\partial I/\partial\lambda$ determines the empirical Landé factor of the 6094.4 Å line to be $+0.29$. This deviates greatly from the LS coupling value of -0.25, but is more in line with expectations from j–j coupling (Landi Degl'Innocenti, private communication). It is however not excluded that the identification of the line is incorrect. In either case, the polarization reveals problems in the atomic data.

If we go on to use the 6093.6 Å line to predict the Landé factor for a line from a different multiplet, 959 Fe I λ6096.7 Å with an LS $g_{\rm eff} = 1.5$ (see Fig. 8), we find instead the much smaller value of 0.58. If we instead assume that the LS value is the right one for this line, we obtain the empirical Landé factors 0.86 and 0.75 for the 6093.6 and 6094.4 Å lines, respectively. In this comparison, however, we have left out the fluxtube physics, which drastically changes the V amplitudes in different ways for different lines. This is the subject of the following sections.

3.4. *Magnetic fluxes, intrinsic field strengths, and area factors*

In our discussion so far, we have avoided the fluxtube physics by using the weak-field approximation presented in Sect. 3.1. A well-known case where this approximation completely fails is the line pair 1 Fe I $\lambda\lambda$5247.06 and 5250.22 Å, which has been discussed extensively in previous papers. Our fully resolved FTS spectra enable us however to use these lines to illustrate the fluxtube physics in a very concrete and direct way.

As the two lines 5247 and 5250 belong to the same multiplet and have equal strength, they should be formed in the same way in the solar atmosphere, the only essential difference being their Landé factors. The weak-field approximation (4) then predicts that their V amplitudes should be in the ratio 2 : 3, but Fig. 9 shows that the ratio is much closer to unity. The explanation is that the Zeeman splitting is no longer small as compared with the line

© European Southern Observatory • Provided by the NASA Astrophysics Data System

1984A&A...131..333S

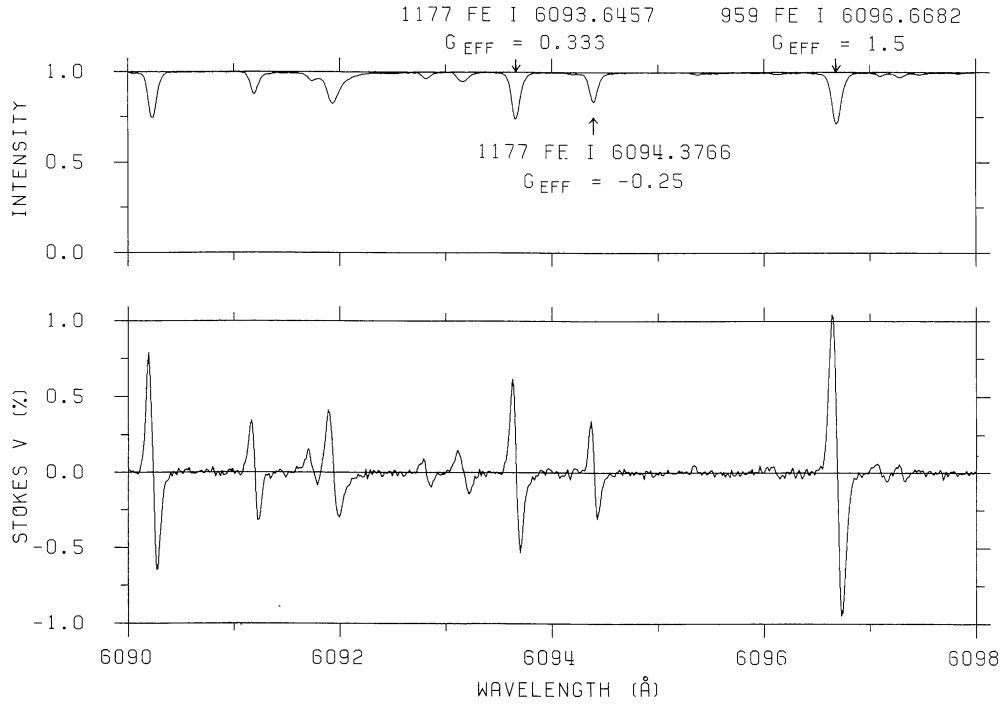

Fig. 8. Stokes *I* and *V* recorded in a strong plage near disk center, illustrating how LS coupling predicts the wrong sign for the Landé factor of the line 1177 Fe I λ6094.38 Å, presuming that the line identification is correct

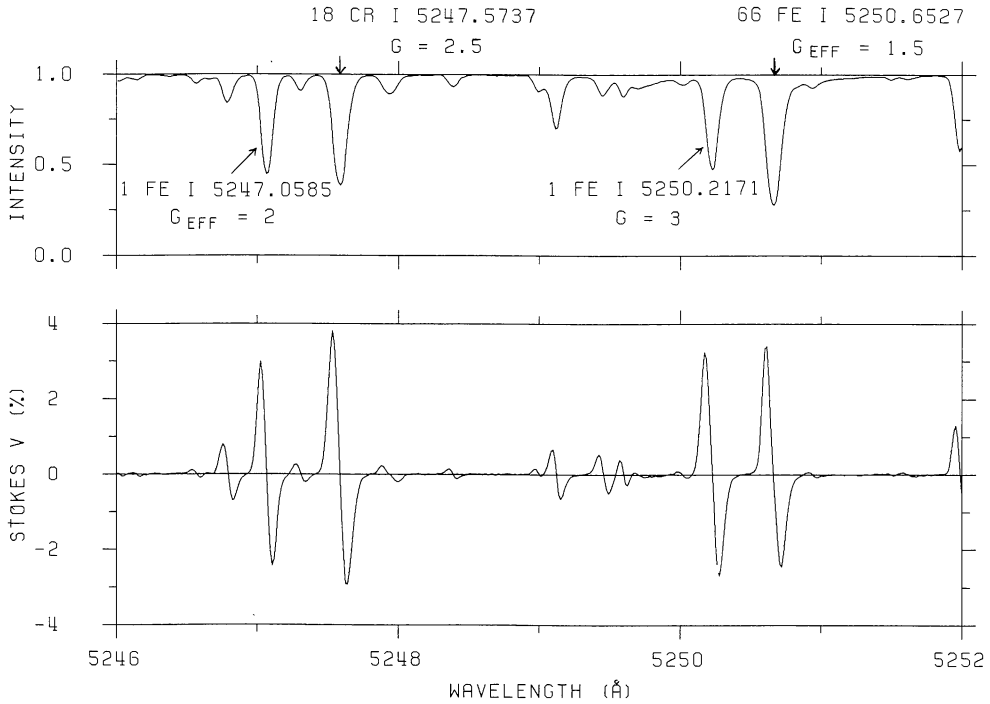

Fig. 9. Stokes *I* and *V* around the 1 Fe I $\lambda\lambda$5247.06 and 5250.22 Å lines in a strong plage near disk center. This line pair has been extensively used in the past to determine the intrinsic field strengths in the spatially unresolved magnetic fluxtubes

width, and therefore the higher-order terms in the Taylor expansion in (4) become important. The dependence on Landé factor is thus no longer linear. It is exactly this non-linearity (Zeeman saturation) that was used a decade ago to determine that the magnetic flux in the quiet-sun network is carried by kG magnetic fields, although the apparent fields seen were only a few G (Stenflo, 1973). This was then achieved by recording the line-wing polarizations simultaneously in the two lines with a Babcock-type magnetograph.

The effect of the higher-order terms in the Taylor expansion is however not only to suppress the *V* amplitude, but also to modify the shape of the *V* profile, mainly by broadening it. The shape of

© European Southern Observatory • Provided by the NASA Astrophysics Data System

1984A&A...131..333S

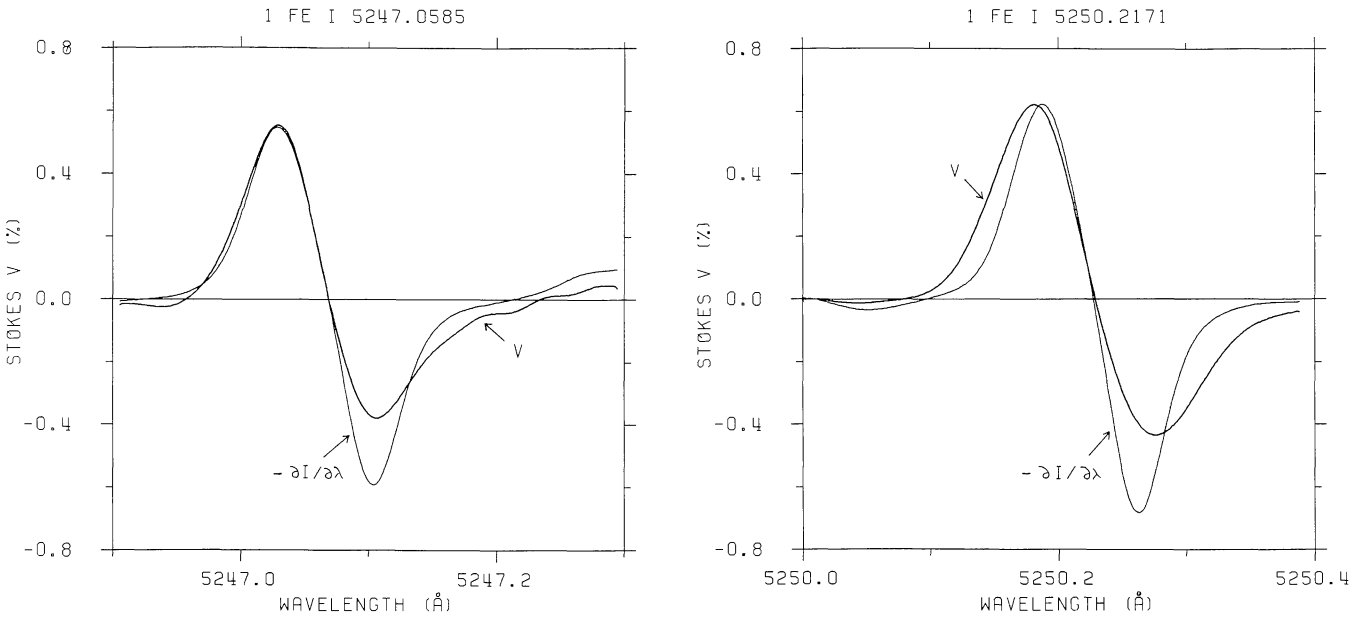

Fig. 10. Stokes V *(thick curves)* and $\partial I/\partial\lambda$ *(thin curves)* around the 5247 and 5250 Å lines, based on data recorded in a weak plage near disk center. The $\partial I/\partial\lambda$ curves have been multiplied by 0.45 mÅ for the 5247 Å line and by 0.53 mÅ for the 5250 Å line, to normalize the amplitudes in the blue line wings to those of the Stokes V curves. Notice the strong broadening of the Stokes V profile for the 5250 Å line as a consequence of the spatially unresolved kG fields. Notice also the pronounced asymmetry between the positive and negative V amplitudes

the V profile will no longer agree with that of the $\partial I/\partial\lambda$ profile, since the linear relation in (4) does not apply any more. That this is indeed the case is shown by Fig. 10. Since the V profiles are strongly asymmetric in the sense that the blue wings have considerably more polarization than the red wings, we should only focus our attention on the blue wings, where the $\partial I/\partial\lambda$ amplitudes have been normalized (the V asymmetries will be discussed in Sect. 3.6). The higher-order terms in (4) are considerably more important in the 5250 Å line because of its larger Landé factor as compared with the 5247 Å line, and this shows up strongly in the broadening of its V profile with respect to $\partial I/\partial\lambda$, whereas the effect in 5247 is very small.

The Zeeman splitting however also broadens the I profile and reduces its depth, and one could therefore expect the resulting difference between V and $\partial I/\partial\lambda$ to be small even when the splitting is large. That the discrepancy nevertheless is large has to do with the different contributions from the spatially unresolved magnetic fine structures. To elucidate this we introduce as our next step a simple-minded two-component model: the fractional area α is covered by fields of strength B, the remaining fraction, $1-\alpha$, is field-free.

The V profile gets its contribution exclusively from the area α, whereas the I profile has contributions from both α and $1-\alpha$. If $\alpha \ll 1$, the contributions become separated: V represents the magnetic region, I the non-magnetic region. In that case the I profile will not be magnetically broadened, which means that the discrepancy between V and $\partial I/\partial\lambda$ can become quite large.

Figure 10 was recorded in the weaker plage where α is small ($\approx 3.3\%$ if we use $B=1$ kG and the fluxtube line-weakening data of Frazier and Stenflo, 1978), and the contributions to V and $\partial I/\partial\lambda$ are therefore well separated. Figure 11 shows the effect of increasing the area factor α when making the recording in the strong plage, where the polarization amplitude (or magnetic flux) is about 8 times larger ($\alpha \approx 25\%$). As the I profile now has a considerable contribution from the magnetic region α as well, the discrepancy between the V and $\partial I/\partial\lambda$ profiles is much smaller. Even the difference caused by the blue-red V asymmetry is greatly reduced. This illustrates how the polarized line profiles provide information on both the intrinsic field strengths and area factors.

To summarize: While the magnetic flux or average field strength

$$\langle B\rangle = \alpha B \tag{6}$$

is determined by the polarization amplitude, the intrinsic field strength B may in principle be determined from a single spectral line by using the *shape* of its V profile, in particular in comparison with the $\partial I/\partial\lambda$ profile. Combining $\langle B\rangle$ and B we obtain the area factor α, which however also directly affects the relation between V and $\partial I/\partial\lambda$ in the case that α is not $\ll 1$.

In reality the problem is however not quite as simple as described, since a difference in width between the V and $\partial I/\partial\lambda$ profiles may also be due to different turbulent and thermal broadening inside and outside the magnetic fluxtubes. Inside the fluxtubes the convective motions are expected to be suppressed, the gas pressure is reduced, and the temperature is changed. These thermodynamic effects will be discussed in the next section. Because of their importance it is not sufficient to use single lines to derive reliable values of the intrinsic field strength B. A carefully selected combination of two or more lines is needed to eliminate the influence of the thermodynamic effects on the determination of B. This has been the philosophy of the line-ratio technique (Stenflo, 1973).

3.5. *Thermodynamic properties of fluxtubes*

The 1 Fe I λ5250.22 Å line was for decades the most commonly used spectral line for observations of solar magnetic fields (von Klüber, 1948). The reasons for choosing this line were:

© European Southern Observatory • Provided by the NASA Astrophysics Data System

1984A&A...131..333S

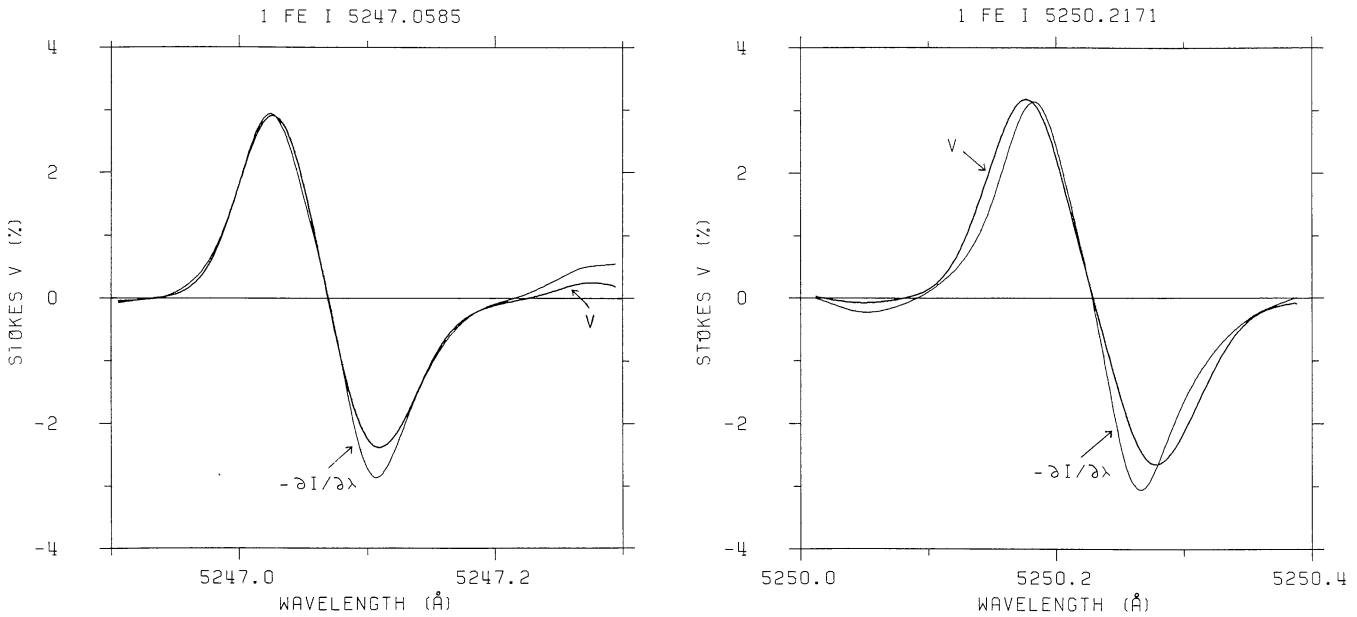

Fig. 11. Same as in Fig. 10, except that it is based on data recorded in a strong plage (same as for Fig. 9). The $\partial I/\partial\lambda$ curves have been multiplied by 3.3 mÅ for the 5247 Å line and by 4.1 mÅ for the 5250 Å line, to normalize the amplitudes in the blue line wings to those of the Stokes V curves. A comparison of Figs. 10 and 11 shows the effect of increasing the magnetic area factor

– It has an unusually large Landé factor ($g=3$), which can be seen by its large Zeeman splitting in sunspots.

– It is unblended and narrow, of intermediate strength.

– It is a normal Zeeman triplet.

Because of its large Landé factor it was (before the end of the 60's) believed that the 5250 Å line should exhibit the largest polarization effects, and that the normal triplet pattern would allow a direct interpretation in terms of magnetic fields.

When inspecting the FTS spectral atlas of the circular polarization, the 5250 Å line does however not catch the eye. The polarization effects are significantly larger in a great number of other spectral lines, although they have considerably smaller Landé factors. As an example, consider the unblended Fe I line immediately beside the 5250.22 Å line in Fig. 9: 66 Fe I λ5250.65 Å. It has a slightly larger polarization amplitude than the 5250.22 Å line. It would thus give magnetograms with the same sensitivity as the 5250.22 Å line, although its Landé factor is smaller by a factor of two. The circumstance that it is not a normal Zeeman triplet is nowadays irrelevant, since the generalization to an anomalous splitting pattern is straightforward and well understood, and does not cause any extra interpretation problems whatsoever (cf. Stenflo, 1971).

There are two reasons why the 5250.22 Å line with its much larger Landé factor does not show more polarization than the 5250.65 Å line: One contributing factor is the Zeeman saturation, which, as we have seen in the preceding section, surpresses the polarization amplitude. This effect is however by far not the whole story, which is immediately apparent by inspecting Fig. 12, where we have plotted I and $\partial I/\partial\lambda$ over the range of interest. Let us compare the 5250.65 Å line with the 5247.06 Å line, for which the Zeeman saturation effect is much less pronounced. Although the $\partial I/\partial\lambda$ amplitude of the 5250.65 Å line is smaller, and although its Landé factor is only 75% of that of the 5247.06 Å line, its polarization amplitude is still larger. This cannot be explained by Zeeman saturation alone but is mainly due to thermodynamic fluxtube effects.

The main thermodynamic effect comes from the temperature difference ΔT between the interior and exterior of the fluxtubes, and its influence on the Saha-Boltzmann population of the atomic energy levels. The effect of a positive ΔT (increased temperature within the fluxtube) is to weaken the spectral lines and thus also correspondingly reduce the polarization amplitudes. These ΔT effects with explicit expressions have been reviewed by Stenflo (1971). The lower the excitation potential χ_e of the lower level of the line, the larger is the ΔT effect. $\chi_e=0.09$ eV for the 5247.06 Å line, 2.20 eV for the 5250.65 Å line. The larger weakening of the 5247.06 Å line explains why its polarization amplitude is not more prominent. For this explanation to work we see that the fluxtube has to be *hotter* than the surroundings at equal optical depth. From this we cannot however draw any direct conclusions about the temperature difference at equal geometrical depth, since the establishment of the geometrical depth scale, dependent on the density reduction in the fluxtube, requires a more sophisticated analysis.

The reason why the $\partial I/\partial\lambda$ spectrum in Fig. 12 is not affected by the line weakening has again to do with the area factor α. Figure 12 represents the weak plage, for which α is small ($\approx 3.3\%$). This means that the $\partial I/\partial\lambda$ spectrum represents almost exclusively the non-magnetic atmosphere, where by definition no line weakening is present. The V spectrum on the other hand has its entire contribution from the line-weakening atmosphere. If we would look at $\partial I/\partial\lambda$ in the strong plage, the situation would be modified as a result of the larger area factor.

Three Fe I lines with surprisingly large polarization amplitudes are shown in Fig. 13. They were recorded in the strong plage strictly simultaneously with the 5247–5250 lines of Fig. 9, so the polarization amplitudes in the two figures can be directly compared. As the lines in Fig. 13 are deeper, their polarization

© European Southern Observatory • Provided by the NASA Astrophysics Data System

1984A&A...131..333S

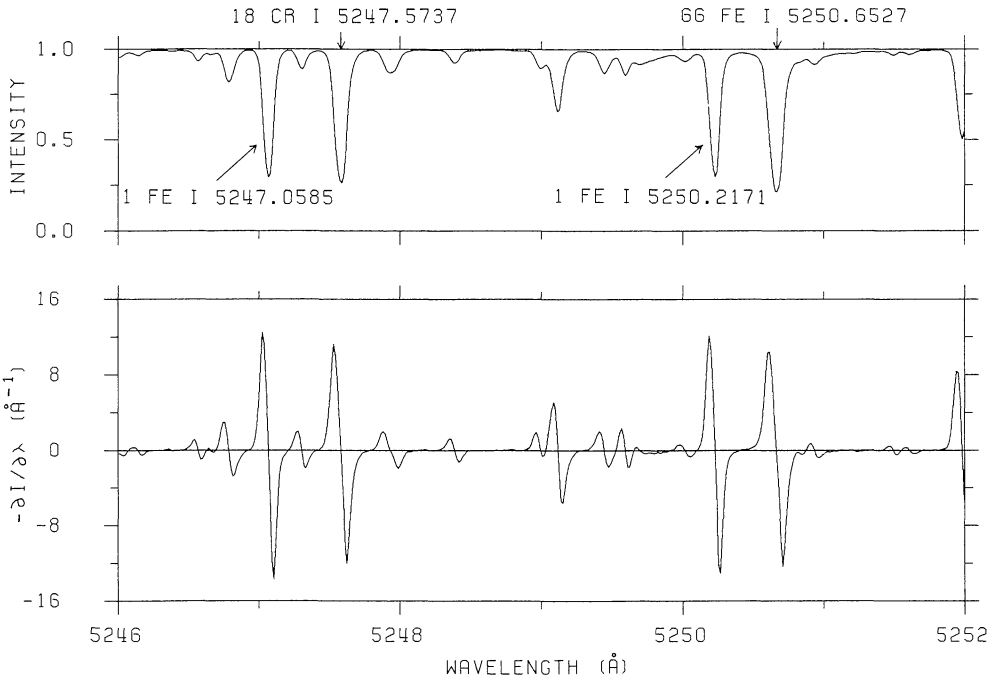

Fig. 12. I and $\partial I/\partial\lambda$ around the 5247 and 5250 Å lines, based on data recorded in a weak plage near disk center. This diagram, in comparison with Fig. 9, illustrates the effect of differential temperature-weakening of the lines inside the fluxtubes. The $\partial I/\partial\lambda$ amplitude of the line 66 Fe I λ5250.65 Å is smaller than that of both the 1 Fe I $\lambda\lambda$5247.06 and 5250.22 Å lines. Although in addition its Landé factor is significantly smaller than that of both of these other lines, its Stokes V amplitude is larger, as a result of less temperature weakening in the fluxtubes

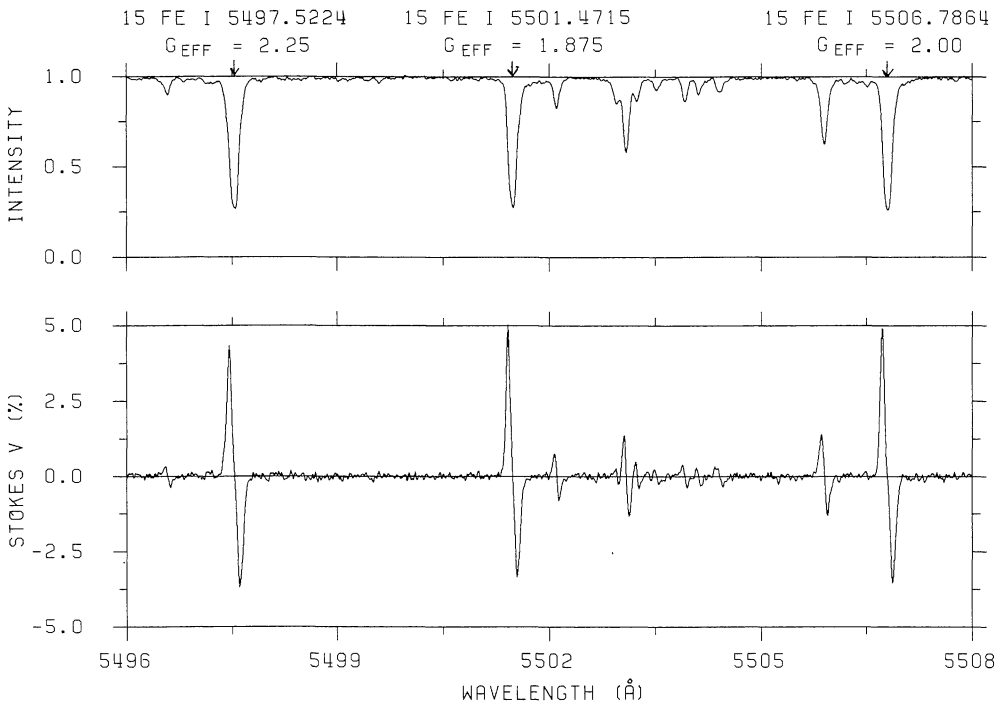

Fig. 13. Stokes I and V of the three lines 15 Fe I $\lambda\lambda$5497.52, 5501.47, and 5506.79 Å, recorded in a strong plage near disk center. All three lines are substantially more polarized than the 5247–5250 Å lines

amplitudes become enhanced, but a comparison with the $\partial I/\partial\lambda$ scale shows that they must also be considerably less temperature weakened, although their χ_e are as low as 0.95–1.01 eV.

Apart from the line weakening there may also be changes in the line broadening and line shape. We would for instance expect more thermal broadening but less turbulent broadening within the fluxtubes. The good agreement between the V and $\partial I/\partial\lambda$ profiles for the 5247 Å line in Fig. 10 indicates however that the net effect of this is small. We also note the excellent agreement between V and $\partial I/\partial\lambda$ for the Na I D_1 and Hβ lines in Figs. 2 and 4. Thus the

© European Southern Observatory • Provided by the NASA Astrophysics Data System

1984A&A...131..333S

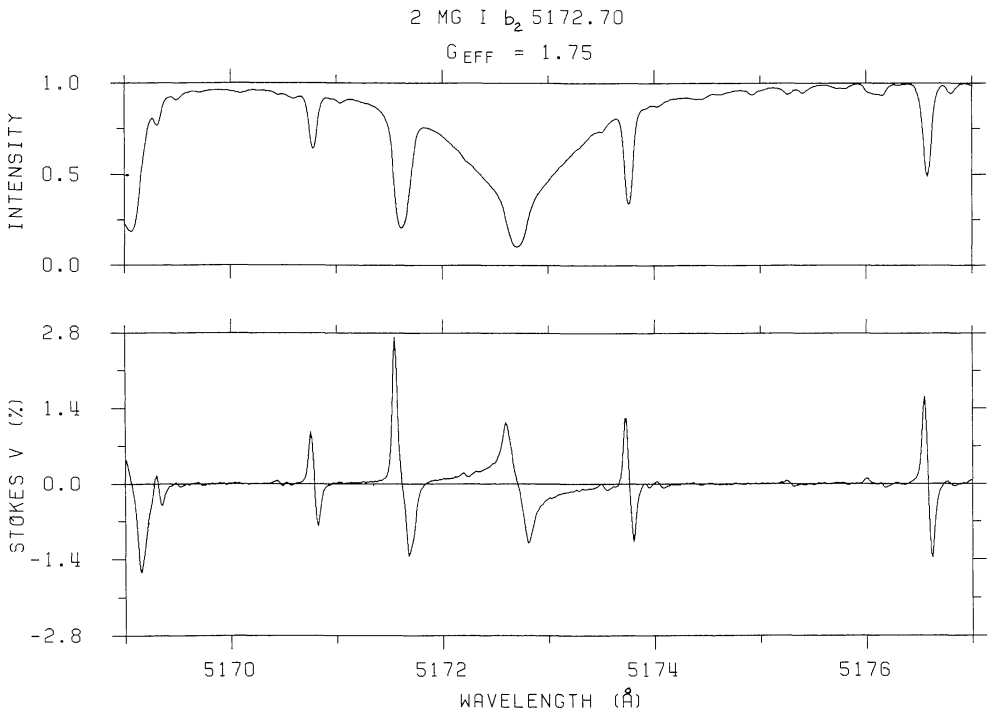

Fig. 14. Stokes I and V around the Mg I b_2 line, recorded in a strong plage near disk center

dominating thermodynamic effects are not on the line width or shape, but on the line strength through changes in the *line depth*.

To summarize: By comparing the V amplitudes of lines of different excitation potential and line strength we may deduce the temperature structure inside the spatially unresolved fluxtubes. Other parameters, like reduced turbulent broadening, give less conspicuous effects but may still be accessible with a more sophisticated numerical evaluation. The pressure and density structure will then follow from the requirements of a self-consistent fluxtube, since B, ΔT, density, etc. are all interconnected in the MHD equations.

There are however additional hurdles to overcome before a fluxtube model can be derived. The most striking demonstration of this are the large red-blue V asymmetries, which show that fluxtubes in magnetohydrostatic equilibrium do not exist on the real sun. This is the topic of the following section.

3.6. *Mass motions inside the fluxtubes*

Our V spectra show a conspicuous profile asymmetry (except for the strongest lines): the polarization amplitude in the blue line wing is considerably larger than that in the red line wing. This asymmetry is not seen in the $\partial I/\partial\lambda$ profiles. In fact the V asymmetry cannot even in principle be reproduced by the $\partial I/\partial\lambda$ profiles. The areas of the blue and red polarization peaks are namely different, not only their amplitudes. For $\partial I/\partial\lambda$ the areas are always the same by definition, since when we integrate $\partial I/\partial\lambda$ over λ, we must retrieve the intensity profile I. If the areas of the blue and red $\partial I/\partial\lambda$ peak were not the same, the integration would result in different continuum levels on the blue and red sides of the line, which we never have.

Had the areas of the blue and red V peaks been equal, we would have had an excellent opportunity to reconstruct the intensity profiles within the fluxtubes. From (4) we see that an integration of V should give I if the Zeeman splitting is known and is much smaller than the line width (which can always be satisfied if we use lines of sufficiently small Landé factor). This derived I profile would then come exclusively from the magnetic area α and represent the fluxtubes alone, uncontaminated by any light from the non-magnetic area $1-\alpha$. The observed area asymmetry in the V profiles shows however that such an integration of V would lead to somewhat unphysical results.

This failure of the "standard" models seems to have far-reaching consequences: In fact it appears to rule out all magneto-hydrostatic fluxtube models. Any static atmosphere would yield fully anti-symmetric V profiles regardless of what unresolved inhomogeneities we introduce. Magnetooptical effects cannot change this, for two reasons: (i) Because of geometrical symmetry at disk center, the statistical average of the magnetic-field *azimuth* angle over the resolution element is zero when we average over the ensemble of much smaller fluxtubes. Therefore Stokes Q and U are also zero. Magnetooptical effects can only enter into Stokes V via Q and U. (ii) The magnetooptical effects in V vanish in the weak-field approximation. Hence the V asymmetry should disappear for lines with small Landé factors, contrary to observations.

The only possible explanation appears to be in terms of *dynamic* models. A mass motion in itself would not give rise to any asymmetry, we need *gradients* in the vertical velocity. At first one may think in terms of horizontal gradients, which would cause line asymmetries when there are correlations between temperature, velocity and magnetic-field fluctuations. This is the way in which the solar granulation introduces asymmetries in the unpolarized intensity profiles. It is true that asymmetries in the V profiles would also be generated this way, but the *areas* of the blue and red V peaks would always remain equal (since you have a linear superposition of differently Doppler-shifted profiles in a multi-component atmosphere, and for each component, which may occupy an infinitesimally small area on the sun, the blue and red V areas are always perfectly balanced). The only remaining possi-

© European Southern Observatory • Provided by the NASA Astrophysics Data System

1984A&A...131..333S

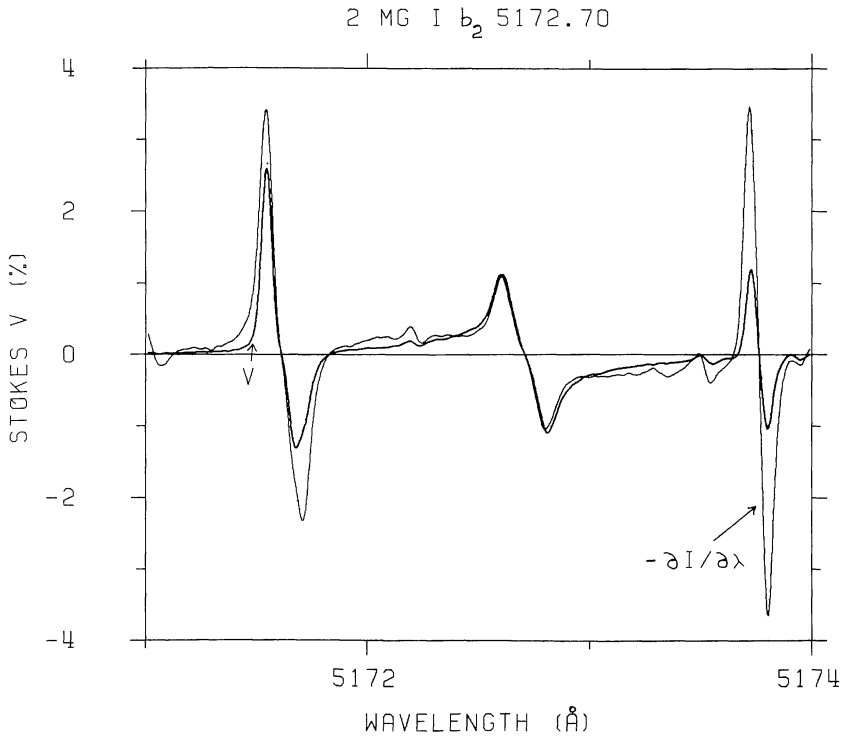

Fig. 15. Stokes V *(thick curve)* and $\partial I/\partial\lambda$ *(thin curve)* around the Mg I b_2 line, using the same data as in Fig. 14. $\partial I/\partial\lambda$ has been multiplied by 4.3 mÅ to normalize the amplitude in the blue wing to that of Stokes V. Notice that the widening of the Stokes V profile with respect to the $\partial I/\partial\lambda$ profile is clearly visible even for such a strong line, thanks to its narrow Doppler core. The use of such strong lines is important for the determination of the fluxtube structure as high as possible in the atmosphere

bility therefore appears to be in terms of *vertical* velocity gradients within the fluxtubes.

A velocity inside the fluxtube relative to the immediate surroundings is also expected to cause a shift of the zero-crossing of the V profile with respect to that of the $\partial I/\partial\lambda$ profile. Figures 2, 4, 10, and 11 show however that this effect is very small, almost zero. The dominating dynamical effect is thus not the Doppler shift itself, but the area asymmetry in the V profile due to the height gradient in the velocity.

Our result of almost zero Doppler shift ($\lesssim 0.1\,\mathrm{km\,s^{-1}}$) of the V zero-crossing is in sharp contrast to the results of Giovanelli and Slaughter (1978), who used the zero-crossing point to derive downflow velocities of the order of $1\,\mathrm{km\,s^{-1}}$ in the fluxtube at photospheric levels, decreasing with height, in contradiction to the expectation from mass conservation (since the density decreases exponentially with height). The V asymmetry causes however an apparent redshift of the V zero-crossing point when the line is not fully spectrally resolved, as is the case in grating spectrometers. The resulting fictitious downdrafts would decrease with height, since the stronger spectral lines formed higher in the atmosphere are broader and have less V asymmetry. In view of our almost non-existent zero-crossing shifts and large asymmetries, it seems that the whole problem of mass motions in fluxtubes, whether updrafts or downdrafts, needs to be reconsidered.

3.7. Height variation of fluxtube parameters

All the fluxtube parameters that we have discussed above, $\langle B\rangle$, B, α, ΔT, $\partial v/\partial z$ (velocity gradient), etc., may be obtained as a function of height in the fluxtube by using lines of different strengths. The height of line formation increases with line strength, but the conversion of line strength to geometrical height depends on the model atmospheres (as well as on the excitation potential and chemical element) used. This conversion therefore has to be coupled to the requirement of having a self-consistent MHD structure of the fluxtube.

To reach as high as possible, one needs to use the strongest lines available. However, since the strongest lines are generally much wider than the weaker ones, the higher-order terms in the Taylor expansion (4), which are essential for the determination of the intrinsic field strength B, become very small. This leads to a greatly increased uncertainty in B for the highest layers. The Balmer lines are for instance much too wide to be useful in the determination of B.

Still there is hope to reach above the temperature minimum. Consider for instance the case of the strong line 2 Mg I b_2 λ5172.70 Å, illustrated in Fig. 14. Its half width is very large because of its strong and extended dispersion wings, but the Doppler core is quite narrow. In Fig. 15 the comparison of the V and $\partial I/\partial\lambda$ profiles shows that the V profile is significantly wider in the Doppler core than the $\partial I/\partial\lambda$ profile, indicating the non-linear effect of a strong, intrinsic magnetic field at the level of formation of the Mg I b_2 line core.

4. Conclusion

The development of the Fourier transform spectrometer into a polarimeter has provided a breakthrough for fluxtube diagnostics. The smearing of the information in the spatial domain, which is unavoidable even with space telescopes, is compensated for by complete resolution in the spectral domain.

With the FTS we can obtain "clean" (uncontaminated by instrumental broadening or straylight) polarized line profiles simultaneously of hundreds of spectral lines of different elements, strengths, excitation potentials, Landé factors, etc. In the diagnostics we are not limited to using selected line pairs (as in the line-ratio technique), but can use a whole set of hundreds of lines to provide simultaneous constraints on a fluxtube model, in a similar manner to the use of 402 unblended Fe I lines by Stenflo and Lindegren (1977) to put constraints on a turbulent magnetic field.

© European Southern Observatory • Provided by the NASA Astrophysics Data System

1984A&A...131..333S

Such a program will be described in a subsequent paper. With this statistical approach it should be possible to derive how the intrinsic field strength, relative fluxtube cross-section (area factor), velocities and thermodynamic properties vary with height inside the fluxtubes.

The polarized FTS spectra also bring several by-products. Empirical Landé factors can be determined, and thereby the validity of LS coupling checked. The polarization helps in the identification of weak lines and blends. In particular all the unpolarized telluric components can be sorted out immediately.

The pronounced asymmetries in the Stokes V profiles apparently cannot be explained within the framework of magnetohydrostatic fluxtube models, but seem to require a vertical velocity with a height gradient within the fluxtubes. These asymmetries would lead to fictitious Doppler redshifts of the zero-crossing point of the V profile when it is not fully resolved with a grating spectrometer.

With the FTS polarimetric recordings becoming a standard procedure, the bottleneck in further progress tends to shift from observations to the handling and analysis of the vast amounts of data recorded in a short time.

To derive empirical fluxtube models, radiative transfer has to be coupled to parameterized, self-consistent MHD models of fluxtubes. In particular the problem of the V asymmetries may only be properly resolved in this way. However, apart from the strongest lines, non-LTE is an unnecessary complication at the present time, since the overwhelming effects are those from fluxtube inhomogeneities in both the horizontal and vertical directions. The remarkable equation (3) shows for instance that we can get quite far even with a minimum of radiative transfer.

For reasons of pedagogical clarity, we have discussed the fluxtubes in terms of a simple-minded two-component model with an area factor α, to bring out the main physical effects. It should however be obvious that for self-consistent MHD models of fluxtubes even a multi-component approach is inappropriate, but that three-dimensional distributions have to be provided. A major problem is to characterize such a three-dimensional model in a self-consistent way using a limited number of free parameters, the values of which will be determined by fitting the spectral data.

References

Baur, T.G., House, L.L., Hull, H.K.: 1980, *Solar Phys.* **65**, 111

Beckers, J.M.: 1969, A Table of Zeeman Multiplets, AFCRL-69-0115

Brault, J.W.: 1978, in Proc. JOSO Workshop Future Solar Optical Observations – Needs and Constraints, G. Godoli, G. Noci, A. Righini, eds., *Osserv. Mem. Oss. Astrofis. Arcetri* No. 106, p. 33

Chandrasekhar, S.: 1950, Radiative Transfer, Clarendon Press, Oxford

Frazier, E.N., Stenflo, J.O.: 1978, *Astron. Astrophys.* **70**, 789

Giovanelli, R.G., Slaughter, C.: 1978, *Solar Phys.* **57**, 255

Harvey, J.W.: 1977, in *Highlights of Astronomy*, E.A. Müller, ed., D. Reidel, Dordrecht, Holland, p. 223

Harvey, J., Livingston, W., Slaughter, C.: 1972, in *Proc. Conf. Line Formation in a Magnetic Field*, NCAR, Boulder, Colorado, p. 227

Klüber, H. von: 1948, *Z. Astrophys.* **24**, 121

Landi Degl'Innocenti, E.: 1982, *Solar Phys.* **77**, 285

Marcy, G.W.: 1983, in Solar and Stellar Magnetic Fields: Origins and Coronal Effects, J.O. Stenflo, ed., IAU *Symp.* **102**, 3

Rachkovsky, D.N.: 1961a, *Izv. Krymsk. Astrofiz. Obs.* **25**, 277

Rachkovsky, D.N.: 1961b, *Izv. Krymsk. Astrofiz. Obs.* **26**, 63

Robinson, R.D., Worden, S.P., Harvey, J.W.: 1980, *Astrophys. J.* **236**, L155

Stenflo, J.O.: 1971, in Solar Magnetic Fields, R. Howard, ed., IAU *Symp.* **43**, 101

Stenflo, J.O.: 1973, *Solar Phys.* **32**, 41

Stenflo, J.O.: 1976, in Basic Mechanisms of Solar Activity, V. Bumba, J. Kleczek, eds., IAU *Symp.* **71**, 69

Stenflo, J.O., Lindegren, L.: 1977, *Astron. Astrophys.* **59**, 367

Stenflo, J.O., Twerenbold, D., Harvey, J.W.: 1983a, *Astron. Astrophys. Suppl. Ser.* **52**, 161

Stenflo, J.O., Twerenbold, D., Harvey, J.W., Brault, J.W.: 1983b, *Astron. Astrophys. Suppl. Ser.* **54**, 505

Stepanov, V.E.: 1958a, *Izv. Krymsk. Astrofiz. Obs.* **18**, 136

Stepanov, V.E.: 1958b, *Izv. Krymsk. Astrofiz. Obs.* **19**, 20

Unno, W.: 1956, *Publ. Astron. Soc. Japan* **8**, 108

© European Southern Observatory • Provided by the NASA Astrophysics Data System